SIMULATION STUDY OF NO_X AND SPECIES FORMATION IN HYDROGEN-AIR DIFFUSION FLAME

Hussam Sadique[1], Arees Qamareen[2], Shah Shahood Alam[3]
Department of Mechanical Engineering, AMU, Aligarh, India
Email:mech.hussam@gmail.com[1], areesq@gmail.com[2], sshaood2004@yahoo.co.in[3]

Abstract

A simulation model of diffusion flame furnace for hydrogen-air was designed and simulated using Ansys Fluent. Results were validated with the experimental result of Fukutani et al. [1] and were in good agreement with the experimental results. Trend of temperature profile shows similar tendency at different heights from burner mouth. Plots of species mole fraction in the flame zone had similar trend and temperature profile shows its peak where H_2 and O_2 gets simultaneously exhausted. Apart from that, velocities at fuel inlet were varied to 10 m/s and 60 m/s and equivalence ratios of 0.66, 0.76 and 0.9 were taken, and results show that at higher velocity and at higher equivalence ratio, NO formation was more, and also at higher equivalence ratio, rate of prompt NO was more. However rate of thermal NO was found to be insignificant. At higher velocity reaction zone was larger so contour of temperature was found to be prolonged and magnitude of maximum temperature was higher in this case and hence NO formation increased significantly.

Index Terms: diffusion flame, equivalence ratio, species, pollutant, prompt

I. INTRODUCTION

In some combustion process fuel and air are moved to the reaction zone and are not initially mixed such flames are known as diffusion or non Premixed type of flame.

Sometimes the gas and air are injected in coaxial parallel tubes and ignited such type of arrangement results in concentric jet flames. In non-Premixed or diffusion flames mixing of gases take place by virtue of molecular or turbulent diffusion.

The diffusion flame occurs at the interface of the gaseous fuel and air and reaction zone thickness increases with time. In diffusion flame the rate of combustion is controlled by the diffusion rate, not by the kinetic rate of reaction. However the mechanism of this flame is very complicated. Industrial gas fired burners, diesel engine, oil fired burners and some gas turbine engine use diffusion flame combustion.

Diffusion flames can be observed in many cases such as when jet of fuel flowing into quiescent air, when two concentric parallel laminar-flowing streams of fuel and oxidizer which forms a laminar diffusion flame, A counter flow diffusion flame.

In concentric jet flames mixing of jet is controlled by using two concentric tubes. Fuel flows in the inner tube and exits to the large concentric tube in which air is flowing. Here velocity in each tube can be adjusted, so the overall fuel to air flow can be adjusted by selecting the cross section area. Here fuel and oxidizer are consumed in flame zone when the fuel-air ratio is sufficient for combustion. The product species and inerts diffuse both inward and outward from the flame zone. Previously Most of the analysis of diffusion flames has been performed based on the flame sheet model proposed by Burke and Schumann [2].

According to this theory the chemical reaction are replaced by single one step overall reaction and this step is assumed as heat releasing step. So all these assumption made in this theory need not be valid in actual diffusion flame. Recent advancement in numerical methods have enabled researchers to approach diffusion flames with detailed mathematical models. Fukutani et al. takes into account the intermediate reaction and several governing equations of fluid mechanics and approaches the problem both experimentally and numerically. In this work a three dimensional modeling is done and it is being simulated in Ansys Fluent. Apart from the work of Fukutani et al. which was concentrated on species profile in flame region and flame structure, in this work with different velocity and at different equivalence ratio, species concentration and NOx prediction has been made.

Nitrogen oxides (NOx), the term used to explain the sum of NO, NO_2, and other oxides of nitrogen, play a major role in the creation of ozone, particulate matter, acid rain. The major sources of man-made NOx emissions are high temperature combustion processes, such as those that occur in automobiles and power plants. In primary, nitrogen oxides (NOx) are divided into the following three categories

Thermal NOx: Forms due to reaction of the atmosphere (molecular) nitrogen and oxygen, the latter formed by splitting of molecular oxygen under high temperature in an oxidation atmosphere. Also called the "Zeldovich" NOx.

Prompt NOx: Reaction of atmosphere (molecular) nitrogen and hydrocarbons or hydrocarbon fragments that originated in the thermal decomposition in a reducing atmosphere. Also called the Fennimore NOx.

Fuel NOx: Formed by the oxidation of nitrogen compounds in the fuel.

In non premixed combustion of hydrocarbons, the first two mechanisms are responsible for the majority of NOx formed.

II. PHYSICAL DESCRIPTION

Experimental setup of Fukutani et al., who studied the flame structure of an axisymmetrical hydrogen-air diffusion flame includes 1 m long and 10 mm wide (in inner diameter) brass pipe, set concentrically inside the Pyrex glass tube of 40 mm in inner diameter. Hydrogen is set to flow inside the brass pipe at a volumetric rate of 30 ml/s and air is pumped into the annular space at a volumetric rate of 143 ml/s. A very stable laminar diffusion flame of Burke-Schumann type with global equivalence ratio of 0.5 was formed. The luminous intensity of the beam was considered homogeneous across its transversal section

III. MATHEMATICAL MODEL

For the three dimensional turbulent flow calculations, the governing equations used in the Cartesian coordinate system are shown below in vector form:

Equation of continuity:

$$\frac{\partial u_i}{\partial x_i} = 0 \tag{1}$$

Equations of momentum:

$$\frac{\partial u_i}{\partial t} + \frac{\partial u_i u_j}{\partial x_i} = -\frac{1}{\rho_l}\frac{\partial P}{\partial x_i} + \frac{\partial}{\partial x_i}\left[\upsilon_e\left(\frac{\partial u_i}{\partial x_j} + \frac{\partial u_j}{\partial x_i}\right)\right] + g_i \tag{2}$$

Where,

$$\upsilon = \upsilon_m + \upsilon_t \tag{3}$$

As shown in Equations. (2) and (3), the effective kinematic viscosity is used to represent the combined effects of molecular and turbulence viscosities.

Equation of Energy:

$$\frac{\partial E}{\partial T} + u_j\frac{\partial E}{\partial x_j} = \emptyset + \frac{1}{\rho}\frac{\partial}{\partial x_j}\left(k.\frac{\partial T}{\partial x_j}\right) \tag{4}$$

Where, E is internal Energy per unit mass

Φ is rate of dissipation of Mechanical Energy per unit mass or called or more often viscous dissipation function per unit mass and is given by

$$\emptyset = \frac{\upsilon}{2}\left(\frac{\partial u_i}{\partial x_j} + \frac{\partial u_j}{\partial x_i}\right)\left(\frac{\partial u_i}{\partial x_j} + \frac{\partial u_j}{\partial x_i}\right) \tag{5}$$

υ is kinematic viscosity

k is coefficient of thermal conductivity

T is temperature

Turbulence Model:

In this study, the K- ε turbulence model was employed to estimate the turbulence viscosity.

Here, turbulence is expressed in terms of the turbulence kinetic energy, K, and its rate of dissipation, ε .the relation between υ_t and the two turbulence characteristics is given by Kolmogorov-Prandtl expression for the turbulent viscosity υ_t

$$\upsilon_t = \frac{C_3 K^2}{\varepsilon} \tag{6}$$

The governing equations for K and ε are shown as follows:

Equation for turbulence kinetic energy

$$\frac{\partial \kappa}{\partial t} + \frac{\partial u_i K}{\partial x_i} = \frac{\partial}{\partial x_i}\left(\frac{\upsilon_t}{\sigma_\kappa}\frac{\partial \kappa}{\partial x_i}\right) + \upsilon_t \frac{\partial u_j}{\partial x_i}\left(\frac{\partial u_i}{\partial x_j} + \frac{\partial u_j}{\partial x_i}\right) - \varepsilon \tag{7}$$

Equation for dissipation rate of turbulence kinetic energy:

$$\frac{\partial \varepsilon}{\partial t} + \frac{\partial u_i \varepsilon}{\partial x_i} = \frac{\partial}{\partial x_i}\left(\frac{\upsilon_t}{\sigma_\varepsilon}\frac{\partial \varepsilon}{\partial x_i}\right) + \frac{C_1 \varepsilon \upsilon_t}{K}\frac{\partial u_j}{\partial x_i}\left(\frac{\partial u_i}{\partial x_j} + \frac{\partial u_j}{\partial x_i}\right) - \frac{C_2 \varepsilon^2}{K} \tag{8}$$

IV. NUMERICAL DETAILS

A three dimensional unstructured tetrahedral mesh was used for numerical simulations. Computational mesh used for this study is shown in Figure 1. A nozzle at the center of the combustor introduces the fuel at certain velocity and at defined inlet temperature.

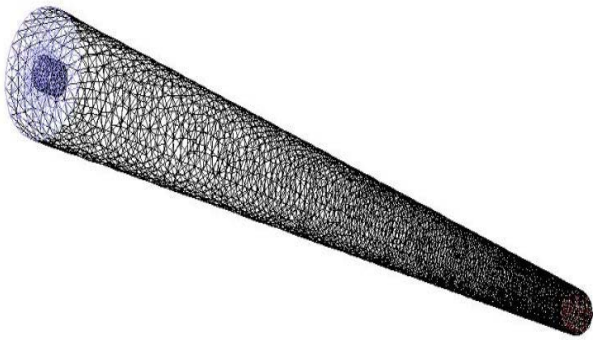

Fig.1 Computational Mesh

V. VALIDATION

This case was taken similar to that of taken by Fukutani et al. [1] and his experimental and simulated results were verified in this work using Ansys Fluent. Fukutani et al. assumed that the flame is axisymmetric, heat transfer from the flame to its surrounding as well as the radiant heat transport inside the flame were neglected, however this assumptions were not made in simulation study.

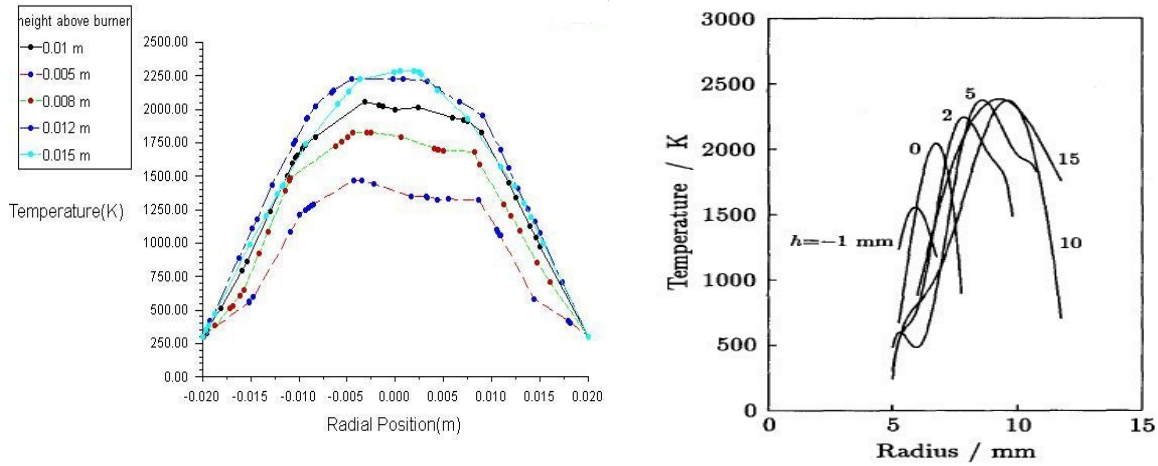

Fig. 2 Variation of temperature with the burner height (a) Simulated Profile (b) Experimental profile

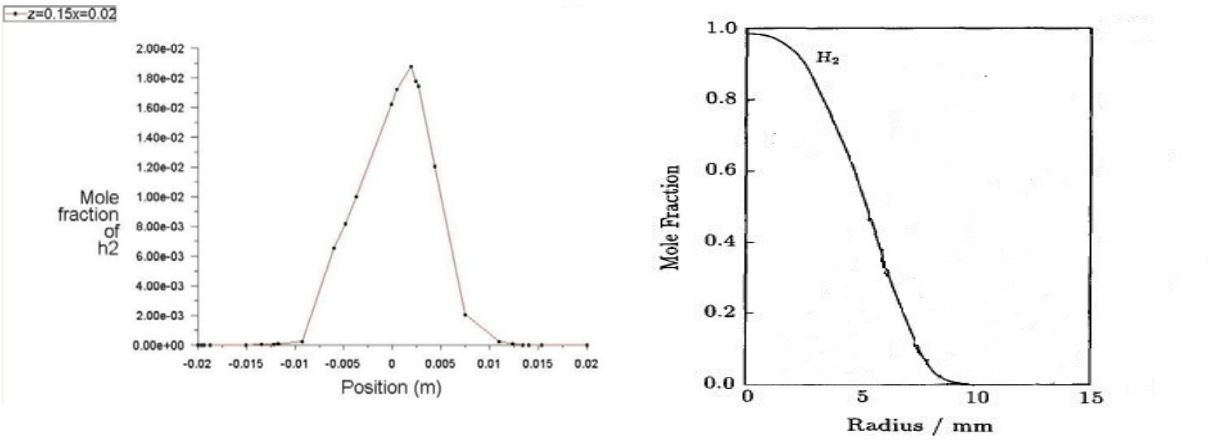

Fig. 3 Variation of mole fraction of H_2 across radius (a) simulated profile (b) Experimental profile

In experimental study fuel volumetric rate was 30 ml/s (velocity=0.3819m/s) and that of air was 143 ml/s (velocity=0.1213 m/s) and overall equivalence ratio was taken as 0.5.
Figure 2 shows the variation of temperature with height from the burner. Simulated profile and experimental profile shows the similar tendency. At very low height experimental data shows the higher temperature than the simulated result this is because in simulated work at lower height no reaction was assumed to be taking place but in case of experimental work, a premixed like flame zone is created at lower height from the burner which is responsible for higher temperature at lower portion.

Figure 3 shows the profile of mole fraction of H_2 and trend of both the profile is similar i.e. at the centre of furnace mole fraction of H_2 is maximum and it diminishes across the radius. Experimental profile is taken as axisymmetric and only half of its portion is being shown. However in the simulated profile, mole fraction of H_2 is less because the profile which is being generated along a particular line falls in the region where H_2 mole fraction is less.

VI. RESULTS AND DISCUSSIONS

The diffusion flame model specification was taken similar to the model used in Fukutani et al. [1] for the study of axisymmetric hydrogen-air diffusion flame. In this study different inlet conditions were taken and detailed study was done

Figure 4 shows the variation of mole fraction of different species at different velocities of fuel. Which shows that at higher velocity flame length would be larger because the span where H_2 and O_2 were exhausted is increased and also temperature will be higher in this case. The mole fraction of H_2O is maximum in the reaction zone, mole fraction of N_2 and O_2 is minimum in this region.

Variation of different parameters were studied when the velocity at fuel inlet was 10 m/s and 60 m/s. Figure 5(a) shows the variation of temperature above the mouth of the burner and Figure 5(b) shows the variation of NO ppm at different height from the burner and at different equivalence ratio. Formation of NO is very much prone to the temperature and this is clearly depicted in these figures. NO ppm is maximum where temperature reaches the maximum value and when the

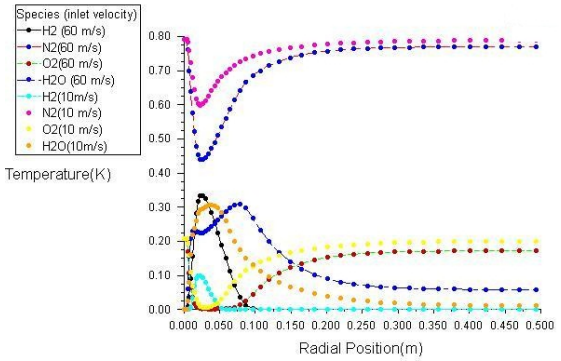

Fig. 4. Species mole fraction at different velocities.

Temperature falls below 400 K, NO formation is suppressed and reaches to zero

When the Equivalence ratio was taken as 0.66 i.e. 50 % of extra air is being supplied then NO formation in this case was minimum because rate of prompt NO formation is least in this case and hence NO formation is minimum in this case. However when

equivalence ratios are taken as 0.76 and 0.9 respectively, rate of prompt NO formation is maximum and thus NO formation is maximum in these cases.

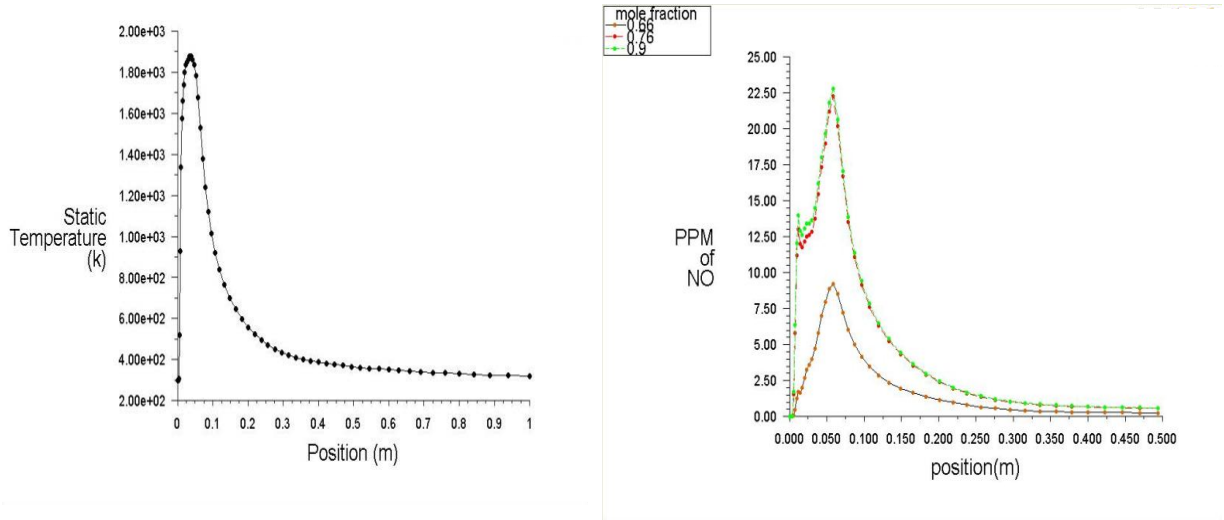

Fig. 5 variation of (a) temperature and (b) NO (ppm) above the burner

Variation of different parameters was studied when the velocity at fuel inlet was increased to 60m/s. Figure 6 shows the variation of temperature and NO ppm respectively above the burner. Temperature is maximum where the O_2 and H_2 are simultaneously exhausted as it is clearly depicted in the figure. NO ppm is maximum in the region where temperature is maximum and compare to previous case when velocity was taken 10m/s, maximum temperature is around 2500 K. Mole fraction of H_2O is maximum in the reaction zone and in this region N_2 mole fraction is low which shows that at higher temperature in this zone it gets converted into NO. At such high temperature O_2 molecule from atmospheric air splits into oxygen and combines with N_2, leads to the formation of NO and further when temperature is less above height 0.2 m from burner N_2 mole fraction goes to maximum.

Figure 7 shows the rate of thermal NO and rate of Prompt NO at different equivalence ratios. When the equivalence ratio is 0.66 then rate of prompt NO is less and when equivalence ratio is 0.76 and 0.9 then its variation is more however as far as rate of thermal NO is concerned the variation is negligible. From Figure 6(b) it is clear that mole fraction of NO is marginally high when equivalence ratio is 0.9 this is because in this case rate of prompt NO is maximum.

VII. CONCLUSION

This simulation work was to study the production of NOx and analysis of various species in a diffusion flame. The simulation estimates both thermal and prompt NOx. This simulation does not involve very complex integration of hundreds of chemical reactions of various species and their intermediates. Such models are highly time consuming and also normally involve heavy computational costs. This simulation was done for Hydrogen fuel. In this simulation maximum NOx prediction, rate of thermal NOx and rate of prompt NOx were also determined at different height of burner and across the radius of flame.

Following conclusion can be made from the study:

(1) At lower velocity of the fuel inlet, maximum temperature was significantly less and hence NOx formation in this case was low and flame length was shorter.

(2) When the velocity was increased enough so that

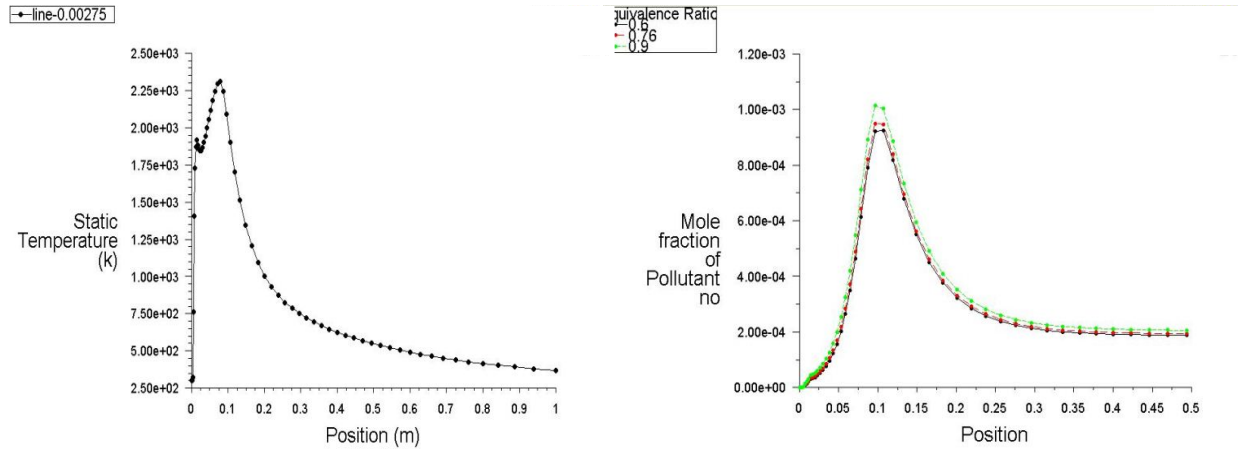

Fig. 6 Variation of (a) temperature and (b) NO ppm above the burner

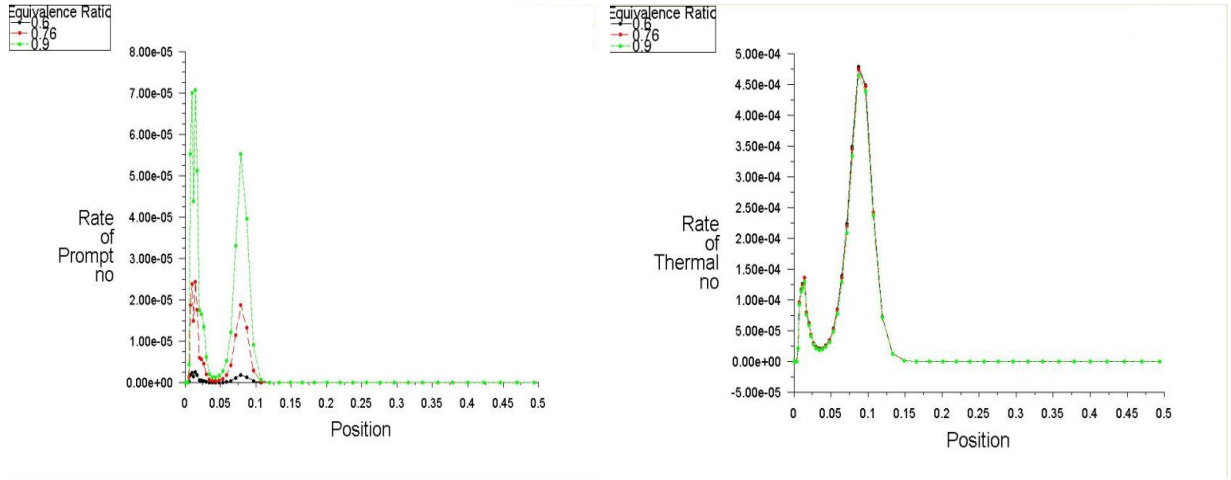

Fig. 7 Variation of (a) Rate of Prompt and (b) rate of Thermal NO

flame attains turbulence then in that case NOx formation and maximum temperature both were higher. Also temperature distribution was further expanded, shows flame length to be longer.

(3) At different equivalence ratio(ϕ) NOx formation was examined and it was found that when ϕ was high and hence air supplied was just close to stoichiometry then rate of prompt NOx was faster as compare to thermal NOx rate.

ACKNOWLEDGMENT

We would like to express grateful thanks to Dr. Santanu De, Assistant Professor, IIT Kanpur , for his support.

REFERENCES

[1] Fukutani, S., Kunioshi, N., and Jinno, H., "Flame Structure of an Axisymmetrical Hydrogen-Air Diffusion Flame," Twenty-Third Symposium (International) on Combustion/The Combustion Institute, 1990/pp. 567-573.

[2] Burke, S. P. and Schunann, T. E. W.: Industrial and Engineering Chemistry 20, 998(1928).

[3] Broman, G.L., Ragland, K.W.,"Combustion Engineering" McGraw-Hill, New York, 1998

[4] Tuteja, A.D., and Newhall, H.K., 1972, "Nitric Oxide formation in Laminar Diffusion Flames," Proceedings of the Symposium on Emissions from Continuous Combustion Systems, General Motor Research Laboratories, Warren, MI, p. 109-122

[5] Ludwig, D.E., Bracco, F.V., Harrje, D.T., "Nitric oxide and composition measurements within diffusion flames around simulated ethanol and ethanol pyridine droplets" Combustion and Flame, volume 25, August–December 1975, Pages 107–120

[6] Fennimore, C. P., 1976, "Effects of Diluents and Mixing on Nitric Oxide from Fuel-Nitrogen Species in Diffusion Flames," Sixteenth Symposium (International) on Combustion, The Combustion Institute, Pittsburg, p. 1065.

[7] Jaasma, D., and Borman, G., 1980, "Peculiarities associated with the Measurement of Oxides of Nitrogen Produced by Diffusion Flames," Combustion Science and Technology, 23, pp. 83-88.

[8] ANSYS Fluent, Release 12.0, ANSYS Inc., 29 Jan. 2009.

[9] Mitchell, R.E., and Sarofim, A.F., 1980, "Nitric Oxide and Hydrogen Cyanide Formation in Laminar Methane/ Air Diffusion Flames," Combustion Science and Technology, 21, pp. 157-167

[10] Turns, S.R., 1995, **"**Understanding NOx Formation in Non Premixed Flames: Experiments and Modeling,**"** Combustion and Flame, 21, pp.361-385.